

## DØ Measurement of the elastic $p\bar{p}$ differential cross section for $0.25 < |t| < 1.2 \text{ GeV}^2$ at $\sqrt{s} = 1.96 \text{ TeV}$

---

**Andrew Brandt**<sup>\*†</sup>

*University of Texas, Arlington*

*E-mail: brandta@uta.edu*

A measurement of the  $p\bar{p}$  elastic differential cross section,  $d\sigma/d|t|$ , is presented as a function of the four-momentum transfer squared,  $|t|$ . The results are obtained from  $\mathcal{L} \sim 30 \text{ nb}^{-1}$  of data collected by the DØ experiment at  $\sqrt{s} = 1.96 \text{ TeV}$  at the Fermilab Tevatron during a two-day period optimized for low  $|t|$  acceptance. In the range  $0.25 < |t| < 0.6 \text{ GeV}^2$  the differential cross section is observed to decay more rapidly than in the range  $0.6 < |t| < 1.2 \text{ GeV}^2$ , where a much more gradual decay is observed. A fit of the form  $d\sigma/d|t| = C \exp -b|t|$ , performed in the range  $0.25 < |t| < 0.6 \text{ GeV}^2$ , yields an exponential slope parameter of  $b = 16.54 \pm 0.10(\text{stat}) \pm 0.80(\text{syst}) \text{ GeV}^{-2}$ .

*XVIII International Workshop on Deep-Inelastic Scattering and Related Subjects*

*April 19 -23, 2010*

*Convitto della Calza, Firenze, Italy*

---

<sup>\*</sup>Speaker.

<sup>†</sup>For the DØ Collaboration (<http://www-d0.fnal.gov>)

## 1. Introduction

The elastic differential cross section,  $d\sigma/d|t|$ ,  $p\bar{p} \rightarrow p\bar{p}$ , contains relevant information about proton structure and non-perturbative aspects of proton ( $p$ )-antiproton ( $\bar{p}$ ) interactions, where  $|t|$  is the four-momentum transfer squared ( $|t| = (p_f - p_i)^2$ ;  $p_i$  and  $p_f$  are the initial and final four-momentum, respectively). The nuclear scattering amplitude dominates the cross section except at very small values of  $|t|$ , and it has been observed that  $d\sigma/d|t|$  has a structure with an exponential decay followed by a dip, the first diffraction minimum, after which  $d\sigma/d|t|$  continues to decrease [1]. The elastic differential cross section plays an important role in constraining phenomenological models which cannot be directly calculated by perturbative QCD [2, 3].

Typical elastic scattering angles are very small (less than a few milliradians), consequently protons and antiprotons scattered at these angles cannot be detected by the main DØ detector [4]. The scattered protons and antiprotons from elastic collisions are therefore detected with specialized detectors inserted within the beam pipe on either side of the interaction point (IP). For Run IIa, the DØ experiment added a Forward Proton Detector (FPD) to measure scattered protons and antiprotons from elastic and diffractive scattering. This note presents a preliminary measurement of the  $p\bar{p}$  elastic differential cross section at  $\sqrt{s}=1.96$  TeV in the range  $0.25 < |t| < 1.2$  GeV<sup>2</sup>, measured using the FPD detector of the DØ experiment. This measurement extends the  $|t|$  range previously studied by the Tevatron experiments CDF [5] and E710 [6], and constitutes a first observation of the first diffraction minimum of  $d\sigma/d|t|$  at Tevatron energies.

## 2. Forward Proton Detector Overview

Figure 1 shows the layout of the FPD (also described in Ref. [4]). In the center of the diagram is the IP surrounded by the DØ detector. The FPD consists of eight quadrupole spectrometers (plus a dipole spectrometer not shown here). The detectors comprising the quadrupole spectrometers are located at about 23 m and 31 m, adjacent to the electrostatic beam separators, on both the proton side (P) and antiproton side (A) and use the Tevatron quadrupole magnets to obtain the scattering angles of the scattered  $p/\bar{p}$  using hits in the scintillating fiber detectors.

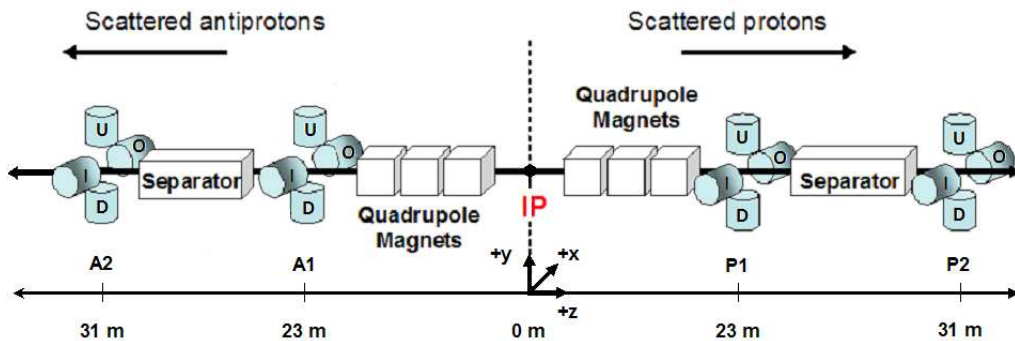


**Figure 1:** The layout of the Roman pot stations and Tevatron components comprising the Forward Proton Detector as described in the text (not drawn to scale).

Each spectrometer consists of a pair of scintillating fiber detectors, in the same plane: either above (U), below (D), on the inner side (I), or on the outer side (O) of the Tevatron Ring. This com-

bination of spectrometers maximizes the acceptance for protons and antiprotons given the available space for locating the detectors. Particles traverse thin steel windows at the entrance and exit of each Roman pot (the stainless steel vessel that houses each detector)[7]. The pots were remotely controlled and moved close to the beam (within a few mm) during stable beam conditions.

### 3. Elastic Analysis

First, the elastic data sample is obtained using elastic triggers. Hits are reconstructed from the fibers that are ON, and the hits are then used to select elastic candidate events. In order to reconstruct the path of the protons and antiprotons through this region of the Tevatron, the detectors are aligned with respect to the beam and then the beam transport matrices are used for track reconstruction. At this point, a Monte Carlo (MC) simulation is introduced to perform corrections for acceptance, detector resolution and beam divergence effects. To obtain the final elastic differential cross section requires efficiency corrections and the subtraction of residual background.

#### 3.1 Data Sample

The data for this analysis were taken in February 2006 in a dedicated store with special conditions designed to facilitate the positioning of the FPD Roman Pots as close to the beam axis as possible. The Tevatron injection tune with the lattice parameter  $\beta^*=1.6$  m at the DØ IP was used instead of the standard  $\beta^*=0.35$  m lattice, and only one proton and one anti-proton bunch were injected. Scraping in the vertical and horizontal planes was performed to remove the halo tails of the beams and the electrostatic separators were turned off for this store. The recorded luminosity was about  $30 \text{ nb}^{-1}$ , divided in two data sets corresponding to different detector positions. Approximately 20 million events were recorded using a special trigger list optimized for diffractive physics, including triggers for elastic, single diffractive, and double pomeron configurations. This analysis is based primarily on the elastic triggers, which comprised about 25% of the total data sample. Elastic candidate events are required to have four hits: one in each of the two detectors in a pair diagonally opposite spectrometers of the detectors: AU-PD and AD-PU are used for this analysis due to their superior  $|t|$  acceptance, compared to AI-PO and AO-PI, which are used for alignment only.

#### 3.2 Monte Carlo Simulation and Acceptance

A stand alone MC program based on the Tevatron transport matrices was used to simulate elastic events in the FPD. The MC includes the 16 quadrupole detector positions and allows study of the geometrical acceptance of the detectors, resolution smearing, alignment, and effects of beam spot and beam divergence at the IP. The generation of events is based on an ansatz function obtained by fitting the  $d\sigma/d|t|$  distribution of the DØ data. The various corrections were studied using signals generated with a wide range of different  $d\sigma/d|t|$  distributions. The variations in the corrections are quoted as systematic uncertainties.

#### 3.3 Selection and Trigger Efficiencies

The effect of both the selection and trigger efficiencies is determined simultaneously resulting in a single efficiency number for each of the four detectors comprising an elastic combination.

To determine the efficiency of a particular detector, an independent trigger that does not include that specific detector was used. Then the hits were reconstructed in the other three detectors. The  $dN/d|t|$  distribution for events with three reconstructed hits is then compared to the the distribution for events with all four hits reconstructed. The ratio of the two distributions give us the efficiency of the detector of interest as a function of  $|t|$ , where  $|t|$  is reconstructed from the coordinates of the opposite side spectrometer. Typical detector efficiencies are in the range of 50% to 70% depending on the detector and trigger condition.

### 3.4 Cross Section Determination

To obtain  $d\sigma/d|t|$  the acceptance (A) and efficiency ( $\epsilon$ ) corrections are applied to each bin of the raw  $dN/d|t|$  and scaled by the integrated luminosity (L):

$$\frac{d\sigma}{d|t|} = \frac{1}{L \times A \times \epsilon} \frac{dN}{d|t|} \quad (3.1)$$

The acceptance correction (A) includes the  $\phi$  acceptance plus the  $|t|$  bin smearing correction. Since the elastic data was taken with different Tevatron conditions as compared to standard DØ experiment operations, the usual algorithms that are ordinarily used to determine luminosity are not appropriate for this data. To determine the integrated luminosity for this data, a method was developed using the ration of the number of inclusive jets for this data period relative to the number from Run IIa [8]. This ratio should be equal to the ratio of the luminosities, given that various factors such as the energy scale are common to the two running periods and accounting for the different vertex factors. The corresponding integrated luminosities for the two data samples used in this analysis are  $18.3 \text{ nb}^{-1}$  and  $12.6 \text{ nb}^{-1}$ , respectively. The uncertainty in the measurement of these luminosities is 13 % and added in quadrature with the 6.1% uncertainty in the luminosity determination of Run IIa, gives an overall normalization error of 14.3%.

### 3.5 Background Subtraction

Halo contamination is the primary source of background to elastic events. Timing information can be used to veto most halo events. To subtract residual background, first the relative amount of tagged and untagged (residual) background can be determined by assuming that events outside the correlation band between the  $p$  and  $\bar{p}$  coordinates are dominated by background. This normalization factor is then used to subtract background inside the correlation band. The amount of background subtracted inside the elastic correlation band is less than 5% of the signal.

## 4. Results

The four measurements of  $d\sigma/d|t|$  (two elastic combinations with two different detector positions) are combined by doing a bin-by-bin weighted average. Figure 2 shows a comparison of the measured DØ  $d\sigma/d|t|$  at  $\sqrt{s} = 1.96$  TeV to the values measured at 1.8 TeV by the Tevatron CDF [5] and E710 [6] experiments. Note that the DØ measurement is in good agreement with the previous measurements in the region of overlap  $0.25 < |t| < 0.6 \text{ GeV}^2$ . An exponential fit to the slope  $b$  of the  $d\sigma/d|t|$  distribution in this range yield  $b = 16.54 \pm 0.10$  (stat)  $\pm 0.80$  (syst)  $\text{GeV}^{-2}$ . A drastic

change in slope in the DØ  $d\sigma/d|t|$  distribution at  $|t| \approx 0.6$  GeV<sup>2</sup> is observed (other experiments have no reported data in this region).

Many sources of systematic uncertainty to the  $d\sigma/d|t|$  measurement have been considered including uncertainties from measurements of detector positions, detector efficiencies, and the ansatz function used in the MC. The largest uncertainty arises from differences observed in the  $d\sigma/d|t|$  slope obtained from different trigger and detector configurations (added in quadrature to the other sources of systematic uncertainties). Finally there is a 14.3% overall normalization uncertainty from the luminosity determination (not shown in the plot).

In conclusion, DØ has measured the elastic differential cross section,  $d\sigma/d|t|$ , at  $\sqrt{s} = 1.96$  TeV over the range  $0.25 < |t| < 1.2$  GeV<sup>2</sup> providing a first measurement of the first diffraction minimum at Tevatron energies.

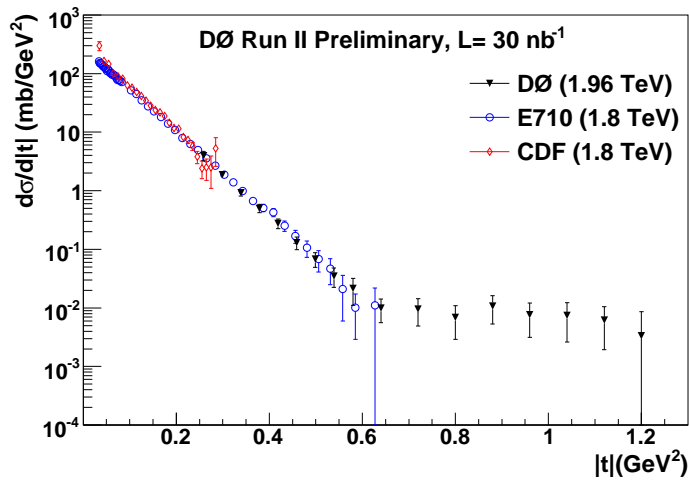


**Figure 2:**  $d\sigma/d|t|$  measured by DØ experiment and compared to CDF and E710 measurements at 1.8 TeV. A normalization uncertainty of 14.3% is not shown. The uncertainties on the points are obtained by adding in quadrature statistical and systematic uncertainties.

## References

- [1] G. Giacomelli, Phys. Rep. **23**, 123 (1976).
- [2] *High Energy Particle Diffraction*, V. Barone, E. Predazzi, Springer, 2002.
- [3] *Quantum Chromodynamics and the Pomeron*, J. Forshaw and D.A. Ross, Cambridge Lectures notes in Physics, 1997.
- [4] M. Abazov *et al.* (D0 Collaboration), Nucl. Instr. and Methods Phys. Res. A **565** 463 (2006).
- [5] F. Abe *et al.* (CDF Collaboration), Phys. Rev. D **50** 5518 (1994).
- [6] N. Amos *et al.* (E710 Collaboration), Phys. Lett. B **247** 127 (1990).
- [7] U. Amaldi *et al.* Phys. Lett. B **44** 112 (1973).
- [8] M. Abazov *et al.* (D0 Collaboration), Phys. Rev. Lett. **101** 062001 (2008).